Resonance-enhanced two-photon dissociation of H$_2$ through nonadiabatically coupled intermediate and final states

Avijit Datta, Samir Saha, and S. S. Bhattacharyya

Atomic and Molecular Physics Section, Department of Materials Science, Indian Association for the Cultivation of Science, Jadavpur, Calcutta 700032, India

Nonperturbative time-dependent calculations of the resonance-enhanced two-photon dissociation probability of H$_2$ in two frequency laser fields from the ground X $^1\Sigma_g^+$ ($v=0$, $j=0$) level to the final continua of GK $^1\Sigma_g^+$ and I $^1\Pi_g$ states have been made as functions of the laser frequencies. The two fields are taken to have linear parallel polarizations with identical sine-squared time dependences of the amplitudes. The first field of frequency ω_1 is near resonant with the two closely spaced excited intermediate levels B $^1\Sigma_u^+$ ($v=14$, $j=1$) and C $^1\Pi_u^+$ ($v=3$, $j=1$), which are strongly coupled to each other through nonadiabatic interaction as well as by radiative Raman coupling. Thus two intermediate levels with mixed Σ^+-Π^+ character are created. The molecule finally dissociates through coherent excitation to a number of near-resonant discrete rovibrational bound levels of $H\bar{H}$ $^1\Sigma_g^+$ and J $^1\Delta_g^+$ embedded into the continua of GK and I states as well as by direct transition to these continua, by absorption of a second photon of frequency ω_2. The nonadiabatic interactions of the bound levels of $H\bar{H}$ and J states, with the respective continuum of GK and I states, give these levels a predissociating character. The interference of the direct transition amplitudes to the continua, and those through the various overlapping predissociating resonances, gives rise to a resultant structure in the dissociation probability with the variation of ω_2. The bound levels used are either (a) a group of three closely spaced vibrational-rotational levels, $H\bar{H}$ $^1\Sigma_g^+$ ($v=4$, $j=0$ and 2), J $^1\Delta_g$ ($v=4$, $j=2$); and (b) the next group of three closely spaced levels, $H\bar{H}$ $^1\Sigma_g^+$ ($v=5$, $j=0$ and 2), J $^1\Delta_g$ ($v=5$, $j=2$). Far from resonance with any predissociating level, the dissociation probability becomes equal to the value obtained by considering only the direct transitions to the continua. For different fixed values of ω_1, the variation of the dissociation probability against ω_2 reflects the characteristics of the excitation of the intermediate resonances with mixed B and C character. On or near resonance, the excitation of the predissociating levels of the J electronic state plays a crucial role in determining the dissociation line shape, whereas the excitation of the predissociating levels of the $H\bar{H}$ electronic state do not affect the dissociation line shape significantly. [S1050-2947(99)03208-4]

PACS number(s): 33.80.Rv, 33.80.Gj

I. INTRODUCTION

The study of dissociation dynamics of small diatomic molecules in laser fields has recently attracted much interest, from both experimental and theoretical points of view [1]. Such studies in the high-intensity range have revealed the presence of a very rich set of highly nonlinear phenomena in molecules. Many of these new phenomena involve the interplay between nuclear and electronic motions on a very short-time scale. Of all the diatomic molecules studied, the hydrogen molecule has always occupied a special place because, being the simplest neutral molecule, it has been used from the beginning to clarify fundamental issues related to molecular dynamics in intense laser fields. At high intensities, however, severe distortion of the electronic charge cloud by the laser field occurs, and this field, in turn, causes strong radiative coupling between a number of these modified electronic states. Thus if different aspects of the behavior of molecular hydrogen are to be related to specific physical interactions, the excitation and dissociation dynamics at lower intensities must be studied. There are still many features of photon-molecule interactions that are not very well understood even for H$_2$, particularly when excited states and their nonadiabatic (NA) coupling are involved. In particular, multiphoton excitations of the molecules with comparatively weak resonant fields to selected set of rovibronic levels, can be used to explore NA interactions between states not accessible by single-photon spectroscopy. In such cases, intense field effects must not be allowed to dominate these interactions so that NA interactions may be able to play a key role in determining the features of the multiphoton transitions. At the same time, whatever effects the radiation fields may have on the structure and dynamics of the system, must be properly accounted for. Thus experiments and theoretical calculations of multiphoton excitation and dissociation of H$_2$ may be useful particularly for investigating spectroscopic properties of excited states.

In two previous works, with these possibilities in view, Banerjee *et al.* [2] reported time-independent perturbative calculations of two-photon resonance-enhanced dissociation cross sections of H$_2$ in weak laser fields via intermediate levels belonging to the B $^1\Sigma_u^+$ and C $^1\Pi_u$ electronic states. Ionization by the two frequency fields was energetically forbidden, and further multiphoton transitions were ignored at the low intensities considered. The calculations were made for linear and circular polarizations of the two-photon fields and for different combinations of initial and intermediate rotational levels. However, it is well known that these two intermediate electronic states are strongly nonadiabatically

coupled [3]. In fact, this knowledge was used to demonstrate interesting effects on resonance-enhanced Raman scattering in H_2 through rovibrational levels of these states close in energy [4]. Again, the structures in the two-photon resonance-enhanced semiperturbative dissociation cross section through levels of the B $^1\Sigma_u^+$ state due to the NA coupling between the continuum state of nuclear motion belonging to GK $^1\Sigma_g^+$ and the embedded bound and quasibound levels of nuclear motions belonging to the $H\bar{H}$ $^1\Sigma_g^+$ and I $^1\Pi_g^+$ electronic states, respectively, were also investigated [5]. The radiative shifts and widths of the intermediate levels belonging to B $^1\Sigma_u^+$ were neglected, and the possible NA coupling of these intermediate resonant levels was absent. Also, the effect of detuning with the intermediate level was not considered. This study concluded that the presence of the predissociating (PD) levels due to the NA coupling generally causes a large increase of the dissociation cross section on resonance, though in a few cases drastic de-enhancements arising from the interference of the transition amplitudes following different paths were also found. Siebbeles *et al.* [6] in their calculation for photodissociation of H_2 from the metastable c $^3\Pi_u^-$ ($v=5$, $j=1$) state by excitation to the quasibound i $^3\Pi_g^+$ ($v=5$, $j=1$ and 2) levels have shown that inclusion of NA coupling of different final electronic states g $^3\Sigma_g^+$, h $^3\Sigma_g^+$, and j $^3\Delta_g$, with the i $^3\Pi_g$ state is essential to reproduce the experimental results [7].

In the present work, we adopt a more realistic nonperturbative time-dependent approach. The H_2 molecule in the X $^1\Sigma_g^+$ ($v=0$, $j=0$) level is dissociated by two synchronized laser pulses with a sine-squared dependence of the field amplitudes on time. The NA coupling between the intermediate near resonant B $^1\Sigma_u^+$ ($v=14$, $j=1$) and C $^1\Pi_u^+$ ($v=3$, $j=1$) levels has been incorporated into the calculation. In fact, these intermediate near-resonant levels have been deliberately chosen so that they become strongly mixed by the NA interaction. For any other choice of intermediate vibrational levels v with rotational quantum number $j=1$ belonging to the B/C electronic states of H_2, the mixing of the levels by NA coupling will be negligible [8]. As we have shown, this coupling plays a very important role in determining the dissociation line shape with respect to both frequencies. Hence the resulting line shape will be very different in the absence of mixing of the intermediate levels. The mixed intermediate levels are coupled by the second laser pulse both to the continua of nuclear motions of GK $^1\Sigma_g^+$ and I $^1\Pi_g^+$ states and the embedded PD levels which now also include, besides the levels of the $H\bar{H}$ $^1\Sigma_g^+$ state, those belonging to the electronic state J $^1\Delta_g^+$. The molecule in the intermediate levels may follow either the direct dissociative paths or the indirect paths through these embedded levels. For the frequencies and intensities used, multiphoton ionization is assumed to be insignificant. The energy-dependent radiative widths and shifts of the intermediate levels as well as the Raman coupling between them have been properly taken into account. The final dissociation line shapes with respect to either of the two frequencies are determined by the interplay of these different radiative and nonradiative couplings. In fact, the radiative coupling of the C $^1\Pi_u^+$ and the J $^1\Delta_g^+$ states, which was not taken into ac-
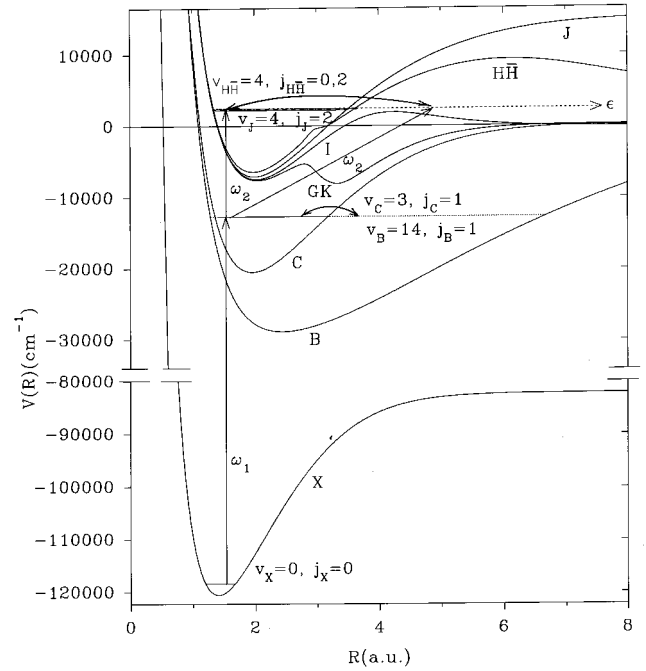

FIG. 1. Adiabatic potential energies $V(R)$ for the pertinent states of H_2. Excitations from the initial ground level of the X state to the two closely spaced nonadiabatically coupled intermediate levels of B and C states, then dissociation to the final GK and I states directly and through predissociating levels of $H\bar{H}/J$ states are shown schematically.

count in any earlier work, has turned out to be very important in determining the line shape. The motivation of the present work is to study the effects of NA coupling between the intermediate B $^1\Sigma_u^+$ and C $^1\Pi_u^+$ states as well as the final $H\bar{H}$ $^1\Sigma_g^+$, GK $^1\Sigma_g^+$, I $^1\Pi_g^+$, and $J^1\Delta_g^+$ states on the two-photon dissociation dynamics of H_2 for realistic laser pulses [9]. To our knowledge, no such calculations were reported earlier.

II. THEORY AND FORMULATION

The scheme for multiphoton dissociation of H_2 molecule that we have considered is shown in Fig. 1 on the pertinent potential-energy diagram. Molecules initially at the $v=0$ and $j=0$ levels of the ground X $^1\Sigma_g^+$ electronic state (which we have designated as $|0\rangle$), successively absorb two photons of frequency ω_1 and ω_2 and dissociate as $H(1s)+H(2s/2p)$, where v and j are the vibrational and rotational quantum numbers, respectively. The intermediate near-resonant levels after absorption of the ω_1 photon are the $v=14$ and $j=1$ levels of B $^1\Sigma_u^+$, designated as $|1\rangle$, and the $v=3$ and $j=1$ levels of C $^1\Pi_u^+$, designated as $|2\rangle$. They have a separation of ~ 17.2 cm^{-1} in the adiabatic Born-Oppenheimer approximation, but are actually strongly coupled through NA interaction [3]. The laser of frequency ω_2 couples both the levels $|1\rangle$ and $|2\rangle$ with the continua of GK $^1\Sigma_g^+$ and I $^1\Pi_g$ states which we denote in general by $|\varepsilon\rangle$. The transition to the dissociative continuum of the EF $^1\Sigma_g^+$ state was earlier shown to be negligible [2,5]. The frequency ω_2 is so chosen that from the levels $|1\rangle$ and $|2\rangle$, after absorption of a ω_2 photon, near resonance occurs with the bound rovibrational

levels of $H\bar{H}\ ^{1}\Sigma_{g}^{+}$ with $j=0$ and 2 (levels $|3\rangle$ and $|4\rangle$, respectively in our notation) and v either 4 or 5 and also with the $j=2$ level of $J\ ^{1}\Delta_{g}^{+}$ (level $|5\rangle$) and v either 4 or 5. These levels are embedded within the continua of GK and I states, and interact nonadiabatically with them to dissociate as $H(1s)+H(2s/2p)$, thus providing new pathways of H_2 photodissociation via these PD levels. The frequency ω_2 is such that ionization is energetically forbidden, and intensity is chosen so that ionization due to further radiative multiphoton transition can be neglected. Other bound levels of $H\bar{H}$ and J states, and the quasibound levels of the I state are highly off-resonant with $|1\rangle$ and $|2\rangle$ and contribute insignificantly to the dissociation dynamics.

The time-dependent Schrödinger equation for the molecular system in the two frequency laser fields is given by (in a.u.)

$$i\frac{\partial|\Psi\rangle}{\partial t}=H|\Psi\rangle=(H_{\mathrm{mol}}+\tilde{V}_{\mathrm{rad}}(t)+\tilde{V}_{na})|\Psi\rangle. \quad (1)$$

The total wave function is expanded as

$$|\Psi\rangle=\sum_{n}C_{n}(t)\exp(-iE_{n}t)|n\rangle$$

$$+\sum_{j=1,2}\int C_{\varepsilon_{j}}(t)\exp(-i\varepsilon_{j}t)|\varepsilon_{j}\rangle d\varepsilon_{j}, \quad (2)$$

where E_{n} is the energy of the nth level ($n=0-5$), and $|\varepsilon_{j}\rangle$ is the jth continuum state corresponding to an energy ε_{j}.

The two continua (with $j=1$ and 2) considered here belong to the GK and I electronic states, respectively.

Putting $\tilde{V}=\tilde{V}_{\mathrm{rad}}(t)+\tilde{V}_{na}$, the equation of motion for the probability amplitudes can be written as

$$\dot{C}_{n}(t)=-i\sum_{m}\tilde{V}_{nm}C_{m}(t)e^{i(E_{n}-E_{m})t}$$

$$-i\sum_{j=1,2}\int\tilde{V}_{n\varepsilon_{j}}C_{\varepsilon_{j}}(t)e^{i(E_{n}-\varepsilon_{j})t}d\varepsilon_{j}, \quad (3)$$

where $\tilde{V}_{nm}=\langle n|\tilde{V}|m\rangle$ is the interaction matrix element between $|n\rangle$ and $|m\rangle$ levels, which is time dependent for radiative interaction but time independent for NA interaction. The radiative interaction is taken to arise from two classical pulsed laser fields $\mathcal{E}_1$ and $\mathcal{E}_2$ of frequencies ω_1 and ω_2 with linear parallel polarizations. Thus the total laser field is

$$\mathcal{E}(t)=\mathcal{E}_{1}(t)\cos(\omega_{1}t)+\mathcal{E}_{2}(t)\cos(\omega_{2}t). \quad (4)$$

The field amplitudes $\mathcal{E}_{1}(t)$ and $\mathcal{E}_{2}(t)$ are both assumed to have a sine-squared time-dependence, a Gaussian-like pulse shape with a pulse duration τ_p and pulse width (full width at half maximum) $\tau_p/2$ [10],

$$\mathcal{E}_{1}(t)=\mathcal{E}_{1}^{0}\sin^{2}(\pi t/\tau_{p}), \quad \mathcal{E}_{2}(t)=\mathcal{E}_{2}^{0}\sin^{2}(\pi t/\tau_{p}), \quad (5)$$

where $\mathcal{E}_{1}^{0}$ and $\mathcal{E}_{2}^{0}$ are peak amplitudes.

The bound $\Sigma/\Pi/\Delta$ state wave function is represented by [4(a),5]

$$|\Lambda vjM\rangle=\left[\frac{(2j+1)}{4\pi}\right]^{1/2}R_{\Lambda vj}(R)(2-\delta_{\Lambda0})^{-1/2}[\psi_{\Lambda}(\vec{r},R)D_{M\Lambda}^{j*}(\phi,\theta,0)\pm(1-\delta_{\Lambda0})\psi_{-\Lambda}(\vec{r},R)D_{M,-\Lambda}^{j*}(\phi,\theta,0)], \quad (6a)$$

and the free Σ/Π state wave function is [5]

$$|\Lambda_{f}kj_{f}M_{f}\rangle=\left[\frac{(2j_{f}+1)}{4\pi}\right]R_{\Lambda_{f}kj_{f}}(R)(i)^{j_{f}}e^{-i\delta_{j_{f}}}(2-\delta_{\Lambda_{f}0})^{-1/2}[\psi_{\Lambda_{f}}(\vec{r},R)D_{M_{f}\Lambda_{f}}^{j_{f}*}(\phi,\theta,0)D_{M_{f}\Lambda_{f}}^{j_{f}}(\phi_{k},\theta_{k},0)$$

$$\pm(1-\delta_{\Lambda_{f}0})\psi_{-\Lambda_{f}}(\vec{r},R)D_{M_{f},-\Lambda_{f}}^{j_{f}*}(\phi,\theta,0)D_{M_{f},-\Lambda_{f}}^{j_{f}}(\phi_{k},\theta_{k},0)]. \quad (6b)$$

$\delta_{\Lambda0}$ and $\delta_{\Lambda_{f}0}$ are simply Kronecker deltas used to write the wave functions in generalized forms with proper normalization of the states. ψ's are the Born-Oppenheimer electronic wave functions with the internuclear separation R as a parameter.

$$R_{\Lambda kj}(R)\underset{R\to\infty}{\sim}\left(\frac{2\mu}{\pi\hbar^{2}k}\right)^{1/2}\frac{\sin\left(kR-\frac{j\pi}{2}+\delta_{j}\right)}{R}.$$

k is the magnitude of the asymptotic wave vector of relative motion of photofragments in the direction (θ_k,ϕ_k) with respect to the space-fixed Z axis along the polarization vector of the linearly polarized light. (R,θ,ϕ) are the coordinates of

internuclear vector with respect to the same set of axes. δ_j is the phase shift of the scattered wave j, and μ is the reduced mass of the photofragments.

The radiative interaction Hamiltonian is of the form

$$\tilde{V}_{\mathrm{rad}}=-\vec{\mathcal{E}}(t)\cdot\vec{d}=-[\mathcal{E}_{1}(t)\cos(\omega_{1}t)+\mathcal{E}_{2}(t)\cos(\omega_{2}t)]\hat{\varepsilon}\cdot\vec{d}, \quad (7)$$

where [4a]

$$\hat{\varepsilon}\cdot\vec{d}=\sum_{\lambda=-1}^{+1}d_{\lambda}D_{0\lambda}^{1*}(\phi,\theta,0).$$

The electron-nuclear rotational matrix elements of the nona-diabatically coupled configuration interaction Hamiltonian are [11]

$$\widetilde{V}^{\Sigma\Sigma}\left[R,\frac{d}{dR}\right]=-\frac{1}{2\mu}\left(A(R)+2B(R)\frac{d}{dR}\right),\qquad(8a)$$

where

$$A(R)=\left\langle\psi_0\left|\frac{d^2}{dR^2}-\frac{L^+L^--\Lambda(\Lambda+1)}{R^2}+\frac{1}{4}(\nabla_1+\nabla_2)^2\right|\psi_0\right\rangle$$

and

$$B(R)=\left\langle\psi_0\left|\frac{d}{dR}\right|\psi_0\right\rangle,$$

$$\widetilde{V}^{\Sigma\Pi^+}(R)=-\frac{1}{2\mu R^2}\{2j(j+1)\}^{1/2}S(R),\qquad(8b)$$

where

$$S(R)=\langle\psi_0|L^+|\psi_{-1}\rangle=\langle\psi_0|L^-|\psi_{+1}\rangle;$$

and

$$\widetilde{V}^{\Delta\Pi}(R)=-\frac{1}{2\mu R^2}[j(j+1)-2]^{1/2}L(R),\qquad(8c)$$

where

$$L(R)=\langle\psi_{+2}|L^+|\psi_{+1}\rangle=\langle\psi_{-2}|L^-|\psi_{-1}\rangle=2.0$$

is independent of R. Using the above equations and operators we can find all the parameters.

The level $|0\rangle$ is near resonant with the closely spaced intermediate levels $|1\rangle$ and $|2\rangle$ by absorption of a photon of frequency ω_1. Similarly, $|1\rangle$ and $|2\rangle$ are near resonant with levels $|3\rangle$, $|4\rangle$, and $|5\rangle$ and resonant with the continua $|\varepsilon_j\rangle$ after absorption of a photon of frequency ω_2. We apply the usual rotating-wave approximation. Following Protopapas and Knight [10(b)] and considering only the resonant and near resonant terms, the coupled equations take the forms

$$\dot{C}_0(t)=-iC_1(t)V_{01}(t)e^{-i\Delta_{10}t}-iC_2(t)V_{02}(t)e^{-i\Delta_{20}t},\qquad(9a)$$

$$\dot{C}_1(t)=-iV_{12}C_2(t)e^{i\Delta'_{12}t}-iV_{13}(t)C_3(t)e^{i\Delta_{13}t}-iV_{14}(t)C_4(t)e^{i\Delta_{14}t}-iV_{10}(t)C_0(t)e^{i\Delta_{10}t}-i\sum_{j=1,2}\int V_{1\varepsilon_j}(t)e^{i\Delta_{1\varepsilon_j}t}C_{\varepsilon_j}(t)d\varepsilon_j,\qquad(9b)$$

$$\dot{C}_2(t)=-iV_{21}C_1(t)e^{i\Delta'_{21}t}-iV_{23}(t)C_3(t)e^{i\Delta_{23}t}-iV_{24}(t)C_4(t)e^{i\Delta_{24}t}-iV_{25}(t)C_5(t)e^{i\Delta_{25}t}-iV_{20}(t)C_0(t)e^{i\Delta_{20}t}$$
$$-i\sum_{j=1,2}\int V_{2\varepsilon_j}(t)e^{i\Delta_{2\varepsilon_j}t}C_{\varepsilon_j}(t)d\varepsilon_j,\qquad(9c)$$

$$\dot{C}_3(t)=-iV_{31}(t)C_1(t)e^{-i\Delta_{13}t}-iV_{32}(t)C_2(t)e^{-i\Delta_{23}t}-i\sum_{j=1,2}\int V_{3\varepsilon_j}e^{i\Delta'_{3\varepsilon_j}t}C_{\varepsilon_j}(t)d\varepsilon_j,\qquad(9d)$$

$$\dot{C}_4(t)=-iV_{41}(t)C_1(t)e^{-i\Delta_{14}t}-iV_{42}(t)C_2(t)e^{-i\Delta_{24}t}-i\sum_{j=1,2}\int V_{4\varepsilon_j}e^{i\Delta'_{4\varepsilon_j}t}C_{\varepsilon_j}(t)d\varepsilon_j,\qquad(9e)$$

$$\dot{C}_5(t)=-iV_{51}(t)C_1(t)e^{-i\Delta_{15}t}-iV_{52}(t)C_2(t)e^{-i\Delta_{25}t}-i\sum_{j=1,2}\int V_{5\varepsilon_j}e^{i\Delta'_{5\varepsilon_j}t}C_{\varepsilon_j}(t)d\varepsilon_j,\qquad(9f)$$

and

$$\dot{C}_{\varepsilon_j}(t)=-iV_{\varepsilon_j1}(t)C_1(t)e^{-i\Delta_{1\varepsilon_j}t}-iV_{\varepsilon_j2}(t)C_2(t)e^{-i\Delta_{2\varepsilon_j}t}-iV_{\varepsilon_j3}C_3(t)e^{-i\Delta'_{3\varepsilon_j}t}-iV_{\varepsilon_j4}C_4(t)e^{-i\Delta'_{4\varepsilon_j}t}-iV_{\varepsilon_j5}C_5(t)e^{-i\Delta'_{5\varepsilon_j}t},\qquad(9g)$$

where $\Delta_{i0}=E_i-E_0-\omega_1$, $\Delta_{ik}=E_i-E_k+\omega_2$, $\Delta'_{il}=E_i-E_l$, $\Delta'_{k\varepsilon_j}=E_k-\varepsilon_j$ (i, $l=1$, 2 and $k=3$, 4, 5, ε_j) and $\widetilde{V}_{01}=V_{01}e^{i\omega_1 t}$, $\widetilde{V}_{13}=V_{13}e^{i\omega_2 t}$, $\widetilde{V}_{1\varepsilon_f}=V_{1\varepsilon_f}e^{i\omega_2 t}$, $\widetilde{V}_{12}=V_{12}$, $\widetilde{V}_{3\varepsilon_f}=V_{3\varepsilon_f}$, etc.

Formally integrating Eq. (9g) for C_{ε_j} and substituting in Eqs. (9b)–(9f), we can eliminate the continuum states to obtain a set of integrodifferential equations for the coefficients C_n ($n=0$–5). As shown by Protopapas and Knight [10(b)], using the Markov approximation, the set of integrodifferential equations can be reduced to ordinary differential equations with a set of coupling parameters. This approximation will be applicable in our case because the pulse time chosen by us is much larger than the time scale of evolution set by these coupling parameters and on this scale the fields vary adiabatically. The final equations in terms of these coupling parameters can be written as

$$\dot{C}_0(t)=-iC_1(t)V_{01}(t)e^{-i\Delta_{10}t}-iC_2(t)V_{02}(t)e^{-i\Delta_{20}t},\qquad(10a)$$

$$\dot{C}_1(t) = -iV_{12}C_2(t)e^{i\Delta'_{12}t} - iV_{13}(t)C_3(t)e^{i\Delta_{13}t} - iV_{14}(t)C_4(t)e^{i\Delta_{14}t} - iV_{10}(t)C_0(t)e^{i\Delta_{10}t} - C_1(t)[\tfrac{1}{2}\gamma_{11} + is_{11}]$$

$$- C_2(t)[\tfrac{1}{2}\gamma_{12} + is_{12}]e^{i\Delta'_{12}t} - C_3(t)[\tfrac{1}{2}\gamma_{13} + is_{13}]e^{i\Delta_{13}t} - C_4(t)[\tfrac{1}{2}\gamma_{14} + is_{14}]e^{i\Delta_{14}t} - C_5(t)[\tfrac{1}{2}\gamma_{15} + is_{15}]e^{i\Delta_{15}t},$$

$$(10b)$$

$$\dot{C}_2(t) = -iV_{21}C_1(t)e^{-i\Delta'_{12}t} - iV_{23}(t)C_3(t)e^{i\Delta_{23}t} - iV_{24}(t)C_4(t)e^{i\Delta_{24}t} - iV_{25}(t)C_5(t)e^{i\Delta_{25}t} - iV_{20}(t)C_0(t)e^{i\Delta_{20}t} - C_1(t)$$

$$\times [\tfrac{1}{2}\gamma_{21} + is_{21}]e^{-i\Delta'_{12}t} - C_2(t)[\tfrac{1}{2}\gamma_{22} + is_{22}] - C_3(t)[\tfrac{1}{2}\gamma_{23} + is_{23}]e^{i\Delta_{23}t} - C_4(t)[\tfrac{1}{2}\gamma_{24} + is_{24}]$$

$$\times e^{i\Delta_{24}t} - C_5(t)[\tfrac{1}{2}\gamma_{25} + is_{25}]e^{i\Delta_{25}t},$$

$$(10c)$$

$$\dot{C}_3(t) = -iV_{31}(t)C_1(t)e^{-i\Delta_{13}t} - iV_{32}(t)C_2(t)e^{-\Delta_{23}t} - C_1(t)[\tfrac{1}{2}\gamma_{31} + is_{31}]e^{-i\Delta_{13}t} - C_2(t)[\tfrac{1}{2}\gamma_{32} + is_{32}]$$

$$\times e^{-i\Delta_{23}t} - C_3(t)[\tfrac{1}{2}\gamma_{33} + is_{33}],$$

$$(10d)$$

$$\dot{C}_4(t) = -iV_{41}(t)C_1(t)e^{-i\Delta_{14}t} - iV_{42}(t)C_2(t)e^{-i\Delta_{24}t} - C_1(t)[\tfrac{1}{2}\gamma_{41} + is_{41}]e^{-i\Delta_{14}t} - C_2(t)[\tfrac{1}{2}\gamma_{42} + is_{42}]$$

$$\times e^{-i\Delta_{24}t} - C_4(t)[\tfrac{1}{2}\gamma_{44} + is_{44}],$$

$$(10e)$$

$$\dot{C}_5(t) = -iV_{52}(t)C_2(t)e^{-i\Delta_{25}t} - C_1(t)[\tfrac{1}{2}\gamma_{51} + is_{51}]e^{-i\Delta_{15}t} - C_2(t)[\tfrac{1}{2}\gamma_{52} + is_{52}]e^{-i\Delta_{25}t} - C_5(t)[\tfrac{1}{2}\gamma_{55} + is_{55}], \quad (10f)$$

where

$$\gamma_{nm} = 2\pi \sum_{j=1,2} \int V_{n\varepsilon_j} V^*_{\varepsilon_j m} \delta(E'_n - \varepsilon_j)d\varepsilon_j \qquad (11a)$$

and

$$s_{nm} = \sum_{j=1,2} P\int \frac{V_{n\varepsilon_j}V^*_{\varepsilon_j m}}{E'_n - \varepsilon_j}d\varepsilon_j, \qquad (11b)$$

where $E'_n = E_n + \omega_2$ for $n = 1$ and 2, and $E'_n = E_n$ for $n = 3$, 4, and 5. P indicates the principal value part of the integral.

The diagonal elements with $m = n$ for $n = 1$ and 2 represent the linewidths (γ_{11}, γ_{22}) and line shifts (s_{11}, s_{22}) of the levels $|1\rangle$ and $|2\rangle$ due to their radiative interactions $V_{n\varepsilon_j} = \tilde{V}_{n\varepsilon_j}e^{-i\omega_2 t}$ with the continua of the GK and I states. These linewidths and line shifts are time dependent, since they depend upon the laser field intensities. The off-diagonal elements s_{12} and γ_{12} represent the real and imaginary parts, respectively, of the Raman-like coupling term between the two levels $|1\rangle$ and $|2\rangle$ introduced by the field ω_2. The diagonal elements for $m = n = 3$, 4, and 5 give the field-independent (and hence time-independent) linewidths (γ_{nn}) and line shifts (s_{nn}) of the levels $|3\rangle$, $|4\rangle$, and $|5\rangle$ arising from their NA interactions ($V_{n\varepsilon_j} = \tilde{V}_{n\varepsilon_j}$) with the continua of GK and I states. The off-diagonal elements s_{1n}, s_{2n} and γ_{1n}, γ_{2n} with $n = 3$, 4, and 5 give the real and imaginary parts of the radiative-nonadiabatic mixed terms, respectively.

It may be noted here that the linewidths (γ_{11}, γ_{22}) and line shifts (s_{11}, s_{22}) of the intermediate levels $|1\rangle$ and $|2\rangle$, the imaginary part (γ_{12}), and the real (s_{12}) part of the Raman-like term between the levels $|1\rangle$ and $|2\rangle$, and also the imaginary (γ_{1n}, γ_{2n}) and real (s_{1n}, s_{2n}) parts (with $n = 3$–5) of the radiative-nonradiative mixed terms, will depend on the

energy-dependent dipole-matrix element $\tilde{V}_{n\varepsilon_j}e^{-i\omega_2 t}$ ($1 \leq n \leq 5$). But the linewidths (γ_{nn}) and line shifts (s_{nn}) of the predissociating levels $|n\rangle = |3\rangle$, $|4\rangle$, and $|5\rangle$ will not be affected by the dipole-matrix element and will be determined by the energy-dependent NA coupling matrix element $\tilde{V}_{n\varepsilon_j}$ ($n = 3$–5). In Sec. IV, we show how these energy-dependent radiative and/or nonradiative matrix elements affect our results.

Equations (10a)–(10f) are solved numerically. From the populations $|C_n(t)|^2$ of the different levels $|n\rangle$ ($n = 0$–5), the dissociation probability $P(t)$ at any time t can be calculated as

$$P(t) = 1 - \sum_{n=0}^{5} |C_n(t)|^2. \qquad (12)$$

III. CALCULATIONS

We have calculated the two-photon dissociation probability of the H_2 molecule for transitions from the initial ground $X\ {}^1\Sigma_g^+$ ($v = 0$, $j = 0$) level to the final $GK\ {}^1\Sigma_g^+ + I\ {}^1\Pi_g$ continuum states via two closely spaced nonadiabatically coupled intermediate levels $B\ {}^1\Sigma_u^+$ ($v = 14$, $j = 1$) and $C\ {}^1\Pi_u^+$ ($v = 3$, $j = 1$) in the presence of two linearly polarized parallel laser fields. For both lasers, the electric fields are supposed to vary with time as a sine-squared function. The Born-Oppenheimer potential energies and the adiabatic corrections to them for the X, B, C, GK, $H\bar{H}$, I, and J states are taken from Wolniewicz and Dressler [12,11(a)] and others [13]. The radial bound and free wave functions for single-well potentials are generated by numerically solving the corresponding radial Schrödinger equation using the Numerov-Cooley method [14(a)]. The bound-state eigenenergies and eigenfunctions for the double-well potential ($H\bar{H}$)

TABLE I. The radiative V_{01}, V_{02}, V_{in}, and nonadiabatic V_{12} matrix elements between the bound levels i and n belonging to different electronic states with $i=1$ and 2 and $n=3$, 4, and 5. The assignments of indices i and n are explained in the text. The units of all V are in cm^{-1}, with I in W/cm^2.

		Group 1		Group 2	
V_{01}	$-6.155[-5]^a\sqrt{I_1}$	V_{13}	$-1.070[-5]\sqrt{I_2}$	V_{13}	$1.266[-5]\sqrt{I_2}$
V_{02}	$1.396[-4]\sqrt{I_1}$	V_{14}	$-9.250[-6]\sqrt{I_2}$	V_{14}	$1.129[-5]\sqrt{I_2}$
V_{12}	-13.06	V_{23}	$-1.450[-5]\sqrt{I_2}$	V_{23}	$-7.320[-5]\sqrt{I_2}$
		V_{24}	$1.598[-5]\sqrt{I_2}$	V_{24}	$3.003[-5]\sqrt{I_2}$
		V_{25}	$-2.068[-4]\sqrt{I_2}$	V_{25}	$5.535[-5]\sqrt{I_2}$

$^a6.155[-5]=6.155\times10^{-5}$.

are obtained using the Numerov-Cooley method modified by Wolneiwicz and Orlikowski [14b]. The NA coupling matrix elements between the electronic states B and C have been taken from Wolniewicz and Dressler [12a] and for $H\bar{H}$-GK and J-I states are obtained from Quadrelli, Dressler, and Wolniewicz [11b]. These values are used to compute the matrix elements between specific bound levels and/or continua belonging to these electronic states by integrating them numerically with the generated vibrational and free-state wave functions. The electric dipole transition moments for X-$B(C)$, $B(C)$-GK, and $B(C)$-$H\bar{H}$ transitions are obtained from Wolniewicz [15], and Wolniewicz and Dressler [16a], and those for $B(C)$-I and C-J are taken from Dressler and Wolniewicz [11(a)] and Wolniewicz [16b]. All the data are interpolated using the cubic spline method [17]. We have solved the six coupled differential equations (10a)–(10f) for the probability amplitudes of the bound levels, using the fourth-order Runge-Kutta method [18] by imposing the initial condition $C_0=1$ and $C_1=C_2=C_3=C_4=C_5=0$ at $t=0$. For capturing the dynamics of the system, the time grid must be small enough so that there is a sufficiently large number of time intervals within each cycle of oscillations caused by the exponential terms in Eqs. (10a)–(10f). The constant time grid in this work is taken to be 12.1 fs, which gives well-converged final results. The pulse time τ_p is taken to be 48.4 ns. The peak field amplitudes of the two lasers used are $\mathcal{E}_1^0=1.0\times10^{-4}$ a.u. (which corresponds to a peak intensity $I_1^0=3.51\times10^8$ W/cm^2) and $\mathcal{E}_2^0=8.0\times10^{-6}$ a.u. (which corresponds to a peak intensity $I_2^0=2.25\times10^6$ W/cm^2). We have chosen these values of laser pulse parameters which are quite reasonable from an experimental point of view, because it is seen that around this peak intensities and pulse time the interplay of the radiative and nonradiative NA interactions becomes most evident. Use of much higher intensities will result in saturation and relatively structureless line shapes, while at lower intensities off-resonant excitation will be ineffective. In this sense, we believe that experiments with similar pulse parameters will be most informative.

IV. RESULTS AND DISCUSSIONS

The six PD levels considered in this work have been divided into two groups. The first group (designated group 1) contains the three PD levels $v=4$, $j=0$, and $j=2$ of the $H\bar{H}$ state and $v=4$ and $j=2$ of the J state, while the second group (designated group 2) contains the other three PD levels

of higher energy $v=5$, $j=0$, and $j=2$ of the $H\bar{H}$ state and $v=5$ and $j=2$ of J state. No other bound level exists between these levels. They are also far from the quasibound levels of the I state, which have not been included. Resonance effects arising from both groups are never simultaneously appreciable, and it is sufficient to include in the calculation only one group separately at a time. We have studied the effect of variation of the second frequency ω_2 so that the final energy is varied from below the group 1 levels to above the group 2 levels. In Table I, we list the radiative interaction matrix elements between the bound levels designated as $|0\rangle$–$|5\rangle$. By the rotating-wave approximation, the matrix elements between the initial level $|0\rangle$ of the X state and the intermediate near-resonant levels $|1\rangle$ and $|2\rangle$ belonging to the B and C states are proportional to $\sqrt{I_1}$ and those between the levels $|1\rangle$ ($|2\rangle$) and $|3\rangle$, $|4\rangle$, and $|5\rangle$ of the $H\bar{H}$ and J states are proportional to $\sqrt{I_2}$, where I_1 and I_2 are the intensities of the first and second fields of frequencies ω_1 and ω_2, respectively. V_{12}, given in Table I, is the intensity-independent matrix element of the NA interaction between levels $|1\rangle$ and $|2\rangle$. All the coupling matrix elements are obtained in the same units (cm^{-1}). It is to be noted that at the peak intensity of the laser pulse we have considered, the radiative matrix elements V_{01} and V_{02} are smaller than the NA coupling matrix element V_{12} by one order of magnitude, while the largest radiative coupling matrix element between the intermediate and predissociating levels at the peak intensity is two orders of magnitude smaller than V_{12}. This ensures coherent excitations of the two intermediate levels $|1\rangle$ and $|2\rangle$.

Table II gives the adiabatic energies and NA linewidths and line shifts of the PD levels of $H\bar{H}$ and J states considered, as well as the coupling terms of these levels with $|1\rangle$ and $|2\rangle$ due to the radiative-NA interaction via the continua of GK and I states. These coupling terms all involve the factor $\sqrt{I_2}$. Only the imaginary parts (γ_{1n}, γ_{2n}) of these mixed interaction terms ($n=3$, 4, and 5 for each group) have been tabulated. The values of the radiative shifts (s_{11}, s_{22}) and real part of second-order Raman-like term ($s_{12}\approx s_{21}$) were also calculated, but found to be totally insignificant at the intensity we have considered. Similarly, the real parts of the second-order radiative-nonadiabatic mixed terms ($s_{in}\approx s_{ni}$ with $i=1$ and 2 and $n=3$, 4, and 5), arising from the principal value integrations, were also found to be insignificant at the intensity considered. The levels $|5\rangle$ are sharper by about 25–100 times than levels $|3\rangle$ or $|4\rangle$. It is also interesting that for levels of the $H\bar{H}$ state these mixed coupling

TABLE II. Adiabatic energies E_n, nonadiabatic linewidths γ_{nn}, line shifts s_{nn}, and the imaginary parts of the radiative-nonadiabatic mixed terms γ_{in}, $i=1$ and 2, of the predissociating levels v_n and j_n, $n=3$, 4, and 5. Level designations are the same as in Table I. The energies E_n are with respect to the adiabatic dissociation threshold of B/C states. I_2 is in W/cm^2.

State	Group	n	v_n	j_n	E_n (cm^{-1})	γ_{nn} (cm^{-1})	s_{nn} (cm^{-1})	γ_{1n} (cm^{-1})	γ_{2n} (cm^{-1})
$H\bar{H}$	1	3	4	0	2274.46	200.3	−20.7	$-2.82[-5]^{a}\sqrt{I_2}$	$-1.80[-5]\sqrt{I_2}$
$H\bar{H}$	1	4	4	2	2405.80	199.5	−18.8	$-2.50[-5]\sqrt{I_2}$	$-8.47[-6]\sqrt{I_2}$
J	1	5	4	2	2188.51	1.85	−2.65	$2.11[-5]\sqrt{I_2}$	$-4.71[-5]\sqrt{I_2}$
$H\bar{H}$	2	3	5	0	3829.44	233.5	−8.22	$4.26[-5]\sqrt{I_2}$	$2.18[-5]\sqrt{I_2}$
$H\bar{H}$	2	4	5	2	3949.44	231.8	−7.28	$3.64[-5]\sqrt{I_2}$	$1.14[-5]\sqrt{I_2}$
J	2	5	5	2	3910.30	9.53	1.55	$-4.46[-6]\sqrt{I_2}$	$3.37[-6]\sqrt{I_2}$

$^{a}2.82[-5]=2.82\times10^{-5}$.

terms have the same order of magnitude as the radiative coupling matrix elements (V_{in}) with the levels of the B/C states considered (Table I). However, for the levels belonging to the J state, the radiative coupling matrix elements with the level of C state are larger than the mixed terms by one order of magnitude.

Figure 2 shows that the radiative decay terms γ_{11}, γ_{22}, and γ_{12} are orders of magnitude lower than the other terms γ_{1n}, γ_{2n}, and γ_{nn} ($n=3-5$) shown in Table II, and they vary considerably when the continuum energy ε is changed by change of ω_2. Over the range of continuum energies in which we are interested, γ_{11} and γ_{22} both vary by more than one order of magnitude (about 30–35 times). As we will show, this variation has important bearing on the dissociation spectrum against ω_2, and hence it must be incorporated in the calculation if we want even a qualitatively correct picture of the dissociation spectrum against ω_2. The variation of γ_{12} is relatively small, varying between $\sim 8.42 \times 10^{-11}I_2$ cm^{-1} and $\sim -4.06\times10^{-11}I_2$ cm^{-1} in the range of continuum energy considered.
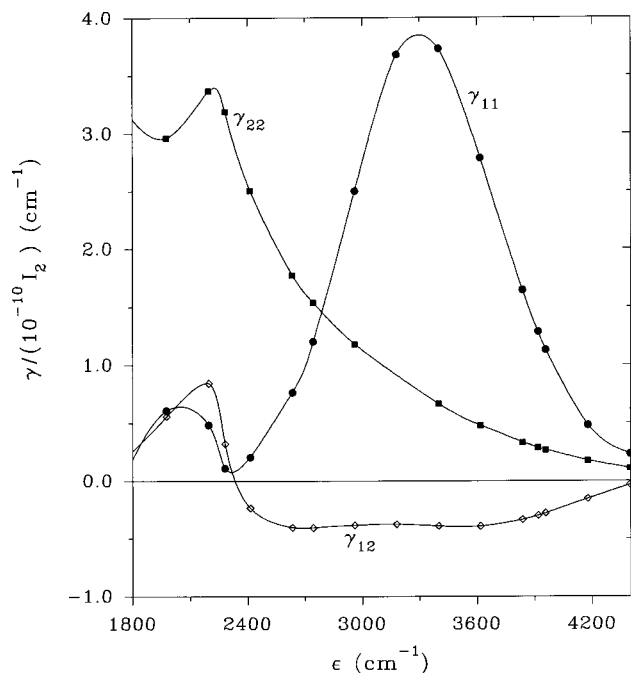

FIG. 2. Variations of γ_{11}, γ_{22}, and γ_{12} with the continuum energy ε measured from the dissociation threshold of the GK/I state.

Figures 3(a) and 3(b) show the plot of the dissociation probability $P(\tau_p)$ against ω_1 when ω_2 is held constant at 14 879 and 16 633 cm^{-1}, respectively. Starting from the $v=0$ and $j=0$ levels of the ground X $^1\Sigma_g^+$ state for the whole range of ω_1 considered, these two values of ω_2 make near resonance with groups 1 and 2 nonadiabatically broadened and shifted PD levels, respectively. The solid and the dashed lines in each case, respectively, represent the dissociation probability with and without considering the NA coupling of the GK and I continua with the embedded bound levels of $H\bar{H}$ and J states. The NA interaction between the two electronic states B and C mixes the two close lying levels $|1\rangle$ and $|2\rangle$, i.e., $v=14$ and $j=1$ of B $^1\Sigma_u^+$ and $v=3$ and $j=1$ of C $^1\Pi_u^+$ states so that two new perturbed eigenstates with mixed Σ^+ and Π^+ characters are created. We interpret the peak at $\omega_1\approx105\,663$ cm^{-1} to be due to a single photon resonance with one of the mixed eigenstates which has about 73% C character and which, for convenience from now on, we will call the perturbed C level [8]. Similarly, the second peak at $\omega_1\approx105\,694$ cm^{-1} is interpreted as due to resonance with the mixed eigenstate with about 73% B character, and henceforth will be called the perturbed B level [8]. The positions of the two perturbed levels thus obtained from the peaks of dissociation probability curves are accurate to about 2 cm^{-1}, and agree well with the very accurate quantum-chemical calculations [8] taking into account all possible intermediate states including continuum. The respective energies of the perturbed B and C levels thus calculated are about $E_1=-12\,683$ cm^{-1} and $E_2=-12\,714$ cm^{-1} with respect to adiabatic dissociation threshold of B/C states. The dissociation process is inefficient when the first excitation step is off-resonance with either of the two perturbed levels, and remains so even in the presence of resonance with the PD levels in the second step. However, significant dissociation is observed for intermediate resonance even in the absence of the PD levels, as shown by the dashed lines. It must be noted here, however, that even in this inefficient dissociation probability far from the individual intermediate resonances, the effect of both the perturbed levels is discernible. This is evident from the line shapes shown in Figs. 3(a) and 3(b). The presence of a single-photon intermediate resonance is expected to exhibit a Lorentzian line shape of the dissociation probability with respect to ω_1. In this case, both the resonances show significant lack of symmetry. Midway between the two peaks the transition probabilities through these two
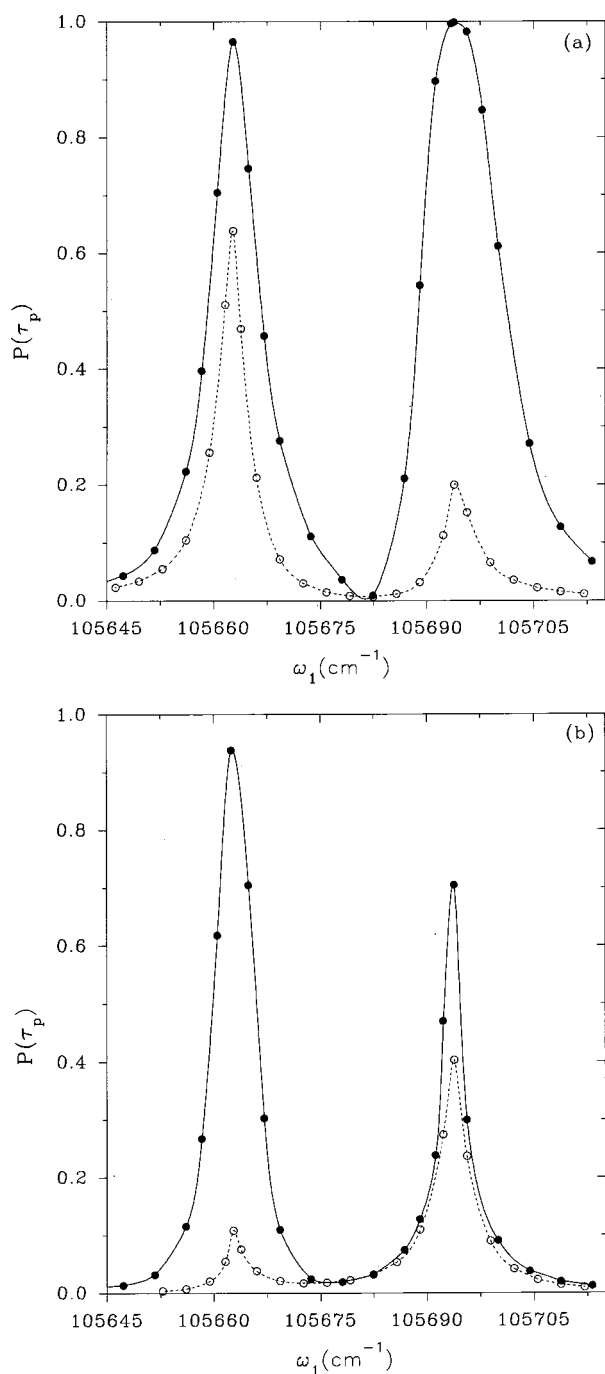
FIG. 3. Dissociation probability $P(\tau_p)$ against ω_1 for (a) ω_2 = 14 879 cm^{-1} and (b) ω_2 = 16 633 cm^{-1}. The solid lines are obtained by considering the nonadiabatic coupling of the predissociating levels. The dashed lines are obtained by ignoring such coupling.

intermediate levels interfere and may cancel each other [most clearly seen in Fig. 3(a)], making both the resonance peaks asymmetric. We can assume that at the far side of each peak the contribution of the other level to the transition amplitude may be neglected. Thus the small radiative linewidths γ_{11} and γ_{22} of the intermediate unperturbed levels can have significant effects. Without the NA coupling of the PD levels, the dissociation probability is higher for resonance with the perturbed C level in Fig. 3(a) and with the perturbed B level in Fig. 3(b). This difference reflects the different contribu-

tions of the adiabatic levels belonging to the perturbed B and C levels in different energy regions due to the variation in their radiative widths. Enhancement of dissociation due to the NA interaction of the PD levels with the continua occurs throughout the range of ω_1 considered, but is most prominent at the peaks. The dissociation probability at the first peak at $\omega_1 \approx 105\,663$ cm^{-1} is enhanced from ~ 0.64 to ~ 0.97, while at the second peak at $\omega_1 \approx 105\,694$ cm^{-1} it is enhanced from ~ 0.20 to ~ 1.0 [Fig. 3(a)]. In Fig. 3(b), the enhancement is from ~ 0.11 to ~ 0.94 for the first peak and from ~ 0.40 to ~ 0.71 for the second peak. The widths of the peaks of dissociation probability increase very significantly when the NA coupling of the PD levels excited by ω_2 is taken into account.

In Figs. 4(a) and 4(b) we plot the dissociation probability $P(\tau_p)$ as function of ω_2 for two different values of ω_1 = 105 694 and 105 663 cm^{-1} corresponding to the resonances with the perturbed B and C levels, respectively. The radiative decay terms γ_{11}, γ_{22}, and γ_{12} are assumed here to remain constant in the range of ω_2 considered. The constant values are equal to the values of these quantities calculated at $\omega_2 = 14\,879$ cm^{-1} for group 1 levels and at ω_2 = 16 633 cm^{-1} for group 2 levels. The change of those parameters with energy has been neglected to ascertain only the role of predissociating resonances in the dissociation process. Over a wider range the energy dependence of the parameters must be taken into account to obtain a quantitatively correct picture of ω_2 dependence of dissociation probability as done in Figs. 5(a)–5(d). In the range of ω_2 shown, the dashed lines have been drawn considering NA coupling of only the two PD levels $v=4$ or 5 and $j=0$ and 2 of $H\bar{H}$ electronic state. In this case, on resonance the dissociation probability is de-enhanced to a slight extent for group 1 levels and is slightly enhanced for group 2 levels. Inclusion of the levels $v=4$ or 5 and $j=2$ of the J electronic state, however, leads to very clear Fano line shapes in each case and very considerable enhancement of the dissociation probability near the peaks as shown by the solid lines. Thus, obviously, the NA coupling of the PD levels belonging to the J electronic state plays the more critical role in determining the dissociation probability in this region of ω_2 compared to the overlapping PD levels of $H\bar{H}$ state which are too diffuse to have prominent resonant characters. In contrast, the PD levels of the J $^1\Delta_g^+$ state are much narrower, and they can be excited much more easily from the C state (as shown in Tables I and II).

The dissociation line shapes with respect to ω_2 calculated by taking into account NA coupling of all the PD levels as well as the proper variation of the radiative decay terms γ_{11}, γ_{22}, and γ_{12} with the continuum energy have been shown in Figs. 5(a)–5(d) by the solid lines for different values of ω_1. In each case, the dashed line gives the dissociation probability neglecting the NA interaction of the PD levels embedded in the continua. In Fig. 5(a), the frequency ω_1 = 105 694 cm^{-1} is chosen such that an intermediate resonance with the perturbed B level occurs. Even in the absence of NA coupling of the PD levels the dissociation probability changes significantly from ~ 0.09 to ~ 0.74 as ω_2 is changed. The peak in this case corresponds to the dissociative continuum energy (ε) position which gives the peak value of
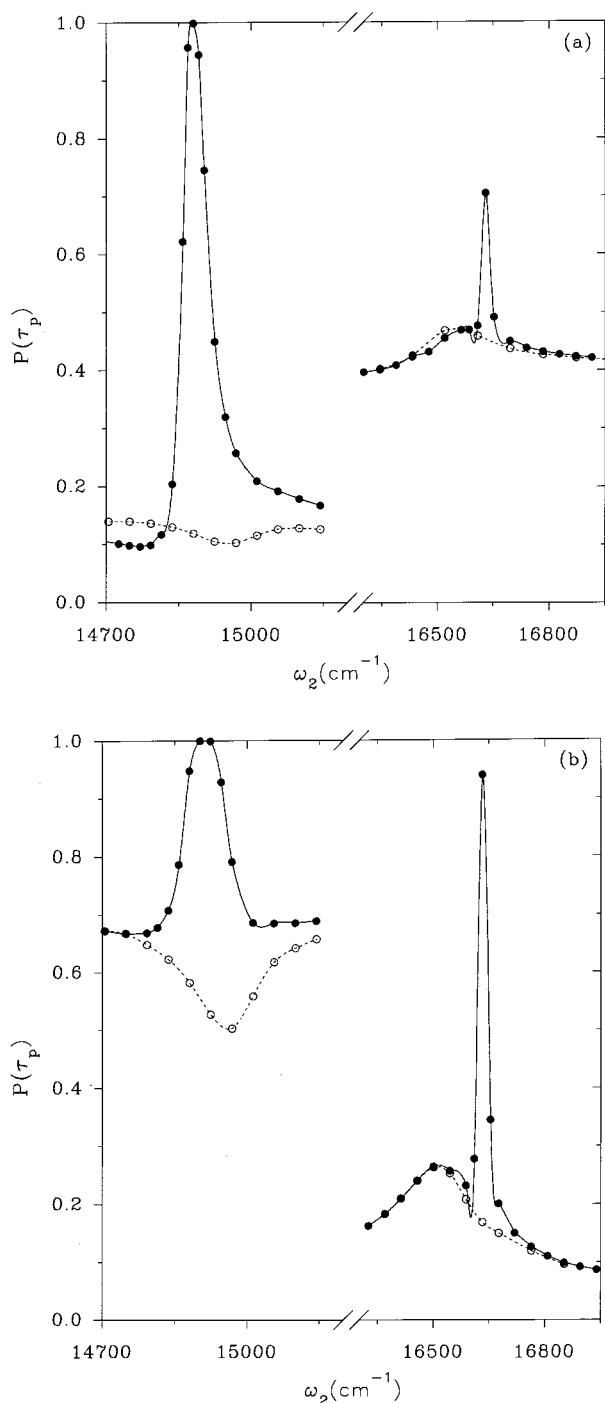
FIG. 4. Dissociation probability $P(\tau_p)$ against ω_2 for (a) $\omega_1 = 105\,694\,\text{cm}^{-1}$ and (b) $\omega_1 = 105\,663\,\text{cm}^{-1}$ with fixed values of γ_{11}, γ_{22}, and γ_{12}. The solid lines are obtained by considering the nonadiabatic coupling of the predissociating levels. The dashed lines are obtained by ignoring such coupling of the predissociating level of the J state.

γ_{11}. This is evident by comparison with Fig. 2. The resonant perturbed B level has $\sim 73\%$ of B character and $\sim 27\%$ of C character [8]. The variation of the dissociation probability with ω_2 is actually due to the combined effect of the variations of γ_{11}, γ_{22}, and γ_{12} with the continuum energy. However, the effect of the variation of γ_{11} is dominant. The effect of the NA interaction between the PD bound levels and the continua is interesting and significant only when the fre-

quency ω_2 is in near resonance with these PD levels, in particular the level belonging to the J state. At the middle range of ω_2, where all the PD levels are far from resonance, the NA effect is insignificant and the dissociation probability tends to the value obtained without considering the NA interaction of the PD levels. In this frequency range the molecule undergoes mainly direct dissociation through the interactions with the continua parametrized by the radiative linewidths. The dissociation line shape for the range $\omega_2 = 14\,500-15\,250\,\text{cm}^{-1}$ is determined by the combined effect of the (group 1) PD levels $v = 4$ and $j = 0$ and 2 of the $H\bar{H}$ state and $v = 4$ and $j = 2$ of the J state. At $\omega_2 \approx 14\,879\,\text{cm}^{-1}$, a prominent Fano-like structure in the dissociation probability is obtained. As shown in Fig. 4(a), the resultant structure is mainly due to the inclusion of the levels $v = 4$ and $j = 2$ of the J state. In the range $\omega_2 = 16\,250-16\,750\,\text{cm}^{-1}$, the resonant enhancement of the dissociation probability is due to the (group 2) PD levels $v = 5$ and $j = 0$ and 2 of the $H\bar{H}$ state and $v = 5$ and $j = 2$ of the J state. At $\omega_2 \approx 16\,601\,\text{cm}^{-1}$, a sharp Fano dissociation line shape is superposed on the direct dissociation probability. Here also it was found from Fig. 4(a) that of all the group 2 levels, it is the one belonging to the J state whose NA interaction with the I state continuum causes the most significant enhancement of the resulting dissociation probability. Although the radiative interaction between the B and J states is forbidden, the fact that inclusion of the PD level of the J state changes the dissociation probability to a large extent at this value of ω_1 indicates that strong mixing of the B and C levels has taken place in the perturbed B level.

In Fig. 5(b), the same quantities as in Fig. 5(a) have been plotted but for $\omega_1 = 105\,689\,\text{cm}^{-1}$, so that the perturbed B level is now near resonant. Understandably, in this case, the dashed line drawn with the absence of the NA coupling of the PD levels shows a much reduced value of dissociation probability but its overall shape remains more or less the same as in Fig. 5(a). The solid line showing the dissociation probability considering the NA effects also has a similar trend as in Fig. 5(a), though with a much decreased value. Here also the two resultant Fano-like structures with peaks at $\omega_2 \approx 14\,884$ and $16\,607\,\text{cm}^{-1}$ can be described due to the NA coupling of both the two groups of the PD levels. The small shifts in the patterns of the peaks compared with those in Fig. 5(a) is due to the small change in ω_1 because the same set of resonant PD levels are excited in both cases.

Figure 5(c) shows the plot of dissociation probability against ω_2 for a value of $\omega_1 = 105\,669\,\text{cm}^{-1}$, so that a near-resonance situation now occurs with the perturbed C level. As before, the dissociation probability plot without consideration of the effect of NA coupling of the PD levels is shown by the dashed line. The perturbed C level has $\sim 73\%$ C character and $\sim 27\%$ B character [8]. This dissociation probability, determined by the variation of γ_{11}, γ_{22}, and γ_{12}, shows two small peaks at the two frequencies ω_2 corresponding to the positions of the peaks in γ_{11} and γ_{22}, respectively, at two different continuum energies in Fig. 2. The effect of the peak in γ_{11} is not as prominent as in Figs. 5(a) and 5(b) because the intermediate level now has a comparatively small mixture of the B level. The solid line indicates that sharp enhancement of the dissociation probability occurs at frequen-
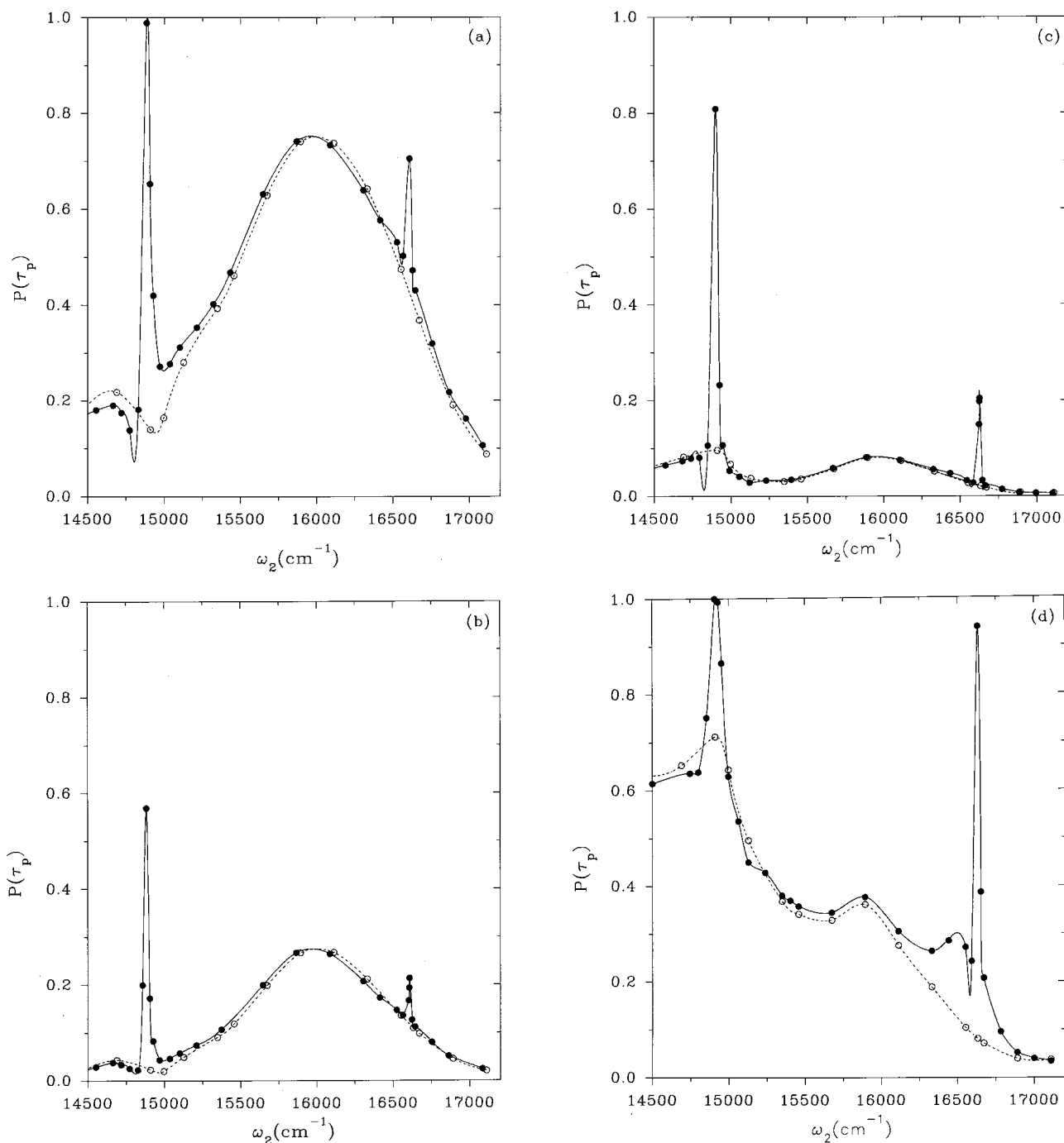
FIG. 5. Dissociation probability $P(\tau_p)$ against ω_2 for (a) $\omega_1 = 105\,694\,\text{cm}^{-1}$, (b) $\omega_1 = 105\,689\,\text{cm}^{-1}$, (c) $\omega_1 = 105\,669\,\text{cm}^{-1}$, and (d) $\omega_1 = 105\,663\,\text{cm}^{-1}$, with the energy-dependent values of γ_{11}, γ_{22}, and γ_{12}. The solid lines are obtained by considering the nonadiabatic coupling of the predissociating levels. The dashed lines are obtained by ignoring such coupling.

cies ω_2, which for this value of ω_1 excite the two groups of PD levels resonantly. These enhancements are sharper than in Fig. 5(b). This is so because the first exciting frequency ω_1 is now nearer to the energy of the perturbed C level, and the intermediate mixed level contains a corresponding greater proportion of C character. The PD level belonging to the J electronic state can be radiatively excited from the C state but not from the B state, and this is the level that has the optimum NA width to have a significant positive effect on the dissociation probability. So the enhancement caused by predissociation becomes more prominent as we approach the

perturbed C level from the perturbed B level by changing ω_1.

In Fig. 5(d), we have an on-resonance situation with the perturbed C level when the first photon has a frequency $\omega_1 = 105\,663\,\text{cm}^{-1}$. The dissociation probability shown by the dashed line has dominantly the pattern of direct dissociation from the C level. The small peak in the range of $\omega_2 = 14\,500 - 15\,250\,\text{cm}^{-1}$ corresponds to the dissociative continuum energy (ε) position which gives the peak value of γ_{22} (Fig. 2). The signature of the presence of the adiabatic B level in the intermediate perturbed C level is the small hump

in the middle, arising due to the peak in γ_{11} curve (Fig. 2) at the corresponding continuum energy. In the range of $\omega_2 = 15\,250 - 16\,250 \text{ cm}^{-1}$, since γ_{11} is about six times larger than γ_{22}, 27% B character is sufficient to produce significant dissociation to make this hump in the dissociation line shape. As before, when the NA coupling of the PD levels is taken into account, the change of the dissociation probability in the range of $\omega_2 = 14\,500 - 15\,250 \text{ cm}^{-1}$ is due to the coherent excitation of the (group 1) PD levels $v=4$ and $j=0$ and 2 of the $H\bar{H}$ state and $v=4$ and $j=2$ of the J state. Similarly, in the range of $\omega_2 = 16\,250 - 15\,750 \text{ cm}^{-1}$, the combined effect of the (group 2) PD levels $v=5$ and $j=0$ and 2 of the $H\bar{H}$ state and $v=5$ and $j=2$ of the J state causes a peak. In both cases it is the level belonging to the J state, which is responsible for the very significant enhancement of the dissociation probability, as is evident from Fig. 4(b). In particular, the excitation of the (group 2) PD levels causes an interesting and significant sharp enhancement of the dissociation probability since the direct dissociation probability (as given by the dashed line) in this region is negligible. We note that the sharpness of the Fano line shapes due to the predissociation resonances is very different from the case shown in Fig. 5(a), stressing that the dissociation line shape is a very sensitive function of ω_1.

V. CONCLUSIONS

We have presented a calculation showing how NA configuration interactions affect two-photon dissociation probability of H_2 in two pulsed laser fields for both on- and off-resonance conditions. The NA interactions are present at two stages of the excitation process. (a) Two closely spaced levels belonging to B and C states are mixed by the NA coupling between these levels, and it is always a mixture of two levels, rather than any one of them, that is excited by the absorption of a photon ω_1. In particular, we have seen that this NA coupling between the intermediate states has an important bearing on the line shape with respect to absorption of photon ω_2, when the energy dependence of the radiative matrix elements between the continuum and intermediate near-resonance levels is taken into account. The radiative mixing, though not negligible, is dominated by the NA mixing at the intensities concerned. This effect of mixing of the intermediate levels is an important feature which emerges from our calculations. The contribution of each of these adiabatic levels to the dissociation probability depends upon the excitation frequency ω_1. (b) The NA interactions between the $H\bar{H}$ and J states, on the one hand, and the GK and I states, on the other hand, make the resonant bound levels,

belonging to the former states and degenerate with the continua of the latter states, predissociating. The NA interactions of the final continuum states with the bound PD levels enhance dissociation on resonance. However, the overlapping PD bound levels influence the dissociation probability in a completely different way depending on their NA widths and radiative coupling with the intermediate resonances. The final result is determined by the coherent excitations of all such levels which are sufficiently near each other and broadened by the NA interactions with the continua. On resonance, with the PD levels, the dissociation line shape is determined by the interference of the transition amplitudes along all the paths. Far from resonance, direct radiative decay from intermediate levels dominates. PD levels $v=4$ or 5 and $j=2$ of the J electronic state generally cause a prominent Fano line shape with a significant enhancement of the dissociation probability at the peak, whereas $v=4$ or 5 and $j=0$ and 2 levels of the $H\bar{H}$ electronic state are very diffuse, and by themselves only cause a much less significant symmetric and broad de-enhancement or enhancement of the dissociation probability.

For photodissociation of H_2 from the $c\ ^3\Pi_u^-$ ($v=5$, $j=1$) level, Siebbeles $et\ al.$ [16] found that while the NA coupling of the quasibound $i\ ^3\Pi_g^+(v=5, j=1)$ level with the $g\ ^3\Sigma_g^+$ ($v=5$, $j=1$) and $h\ ^3\Sigma_g^+$ ($j=1$) states does not have significant effect on the photodissociation cross sections, the NA coupling of the $i\ ^3\Pi_g^-$ ($v=5$, $j=2$) quasibound level with the $j\ ^3\Delta_g^-$ ($v=4$, $j=2$) level greatly enhances the agreement between the theory and experimental results of photodissociation cross sections. In our present calculation of two-photon dissociation probability, we have not found significant effect of the NA coupling of the $H\bar{H}\ ^1\Sigma_g^+$ ($v=4, 5, j=0, 2$) levels with the $GK\ ^1\Sigma_g^+$ continuum on the dissociating probability, whereas NA coupling of the $J\ ^1\Delta_g^+$ ($v=4, 5, j=2$) levels with the $I\ ^1\Pi_g^+$ continuum plays a very prominent role. Similar conclusions about the effect of NA coupling on the dissociation cross sections and probabilities are obtained in the two cases because of the similarity of the dynamics and potential-energy curves of the singlet and triplet states. However, it may be pointed out here that unlike the NA mixing between the intermediate $C\ ^1\Pi_u^+$ and $B\ ^1\Sigma_u^+$ states in our work, there is no NA coupling between the $c\ ^3\Pi_u^-$ and $b\ ^3\Sigma_u^+$ states in the work of Siebbeles $et\ al.$ [6]. We hope that experiments with values of laser parameters similar to those we have used will soon be feasible. The interplay of such experiments and further theoretical work must reveal many of new features and enhance our understanding about the dynamics of excited states of molecules like H_2.

[1] A. Giusti-Suzor, F. H. Mies, L. F. DiMauro, E. Charron, and B. Yang, J. Phys. B **28**, 309 (1995); S. S. Bhattacharyya, in *Atomic and Molecular Physics*, edited by S. P. Khare, Deo Raj, and Ashok Kumar (Bindra, Ghaziabad, 1995), p. 36; A. Datta, S. Saha, and S. S. Bhattacharyya, J. Phys. B **30**, 5754 (1997).

[2] S. Banerjee, M. K. Chakrabarty, S. S. Bhattacharyya, and S. Saha, J. Chem. Phys. **95**, 1608 (1991); **96**, 4974 (1992).

[3] P. S. Julienne, Mol. Phys. **48**, 508 (1973); A. L. Ford, J. Mol. Spectrosc. **53**, 364 (1974).

[4] (a) S. Banerjee, S. S. Bhattacharyya, and S. Saha, J. Raman Spectrosc. **24**, 317 (1993); (b) S. Ghosh, S. S. Bhattacharyya, and S. Saha, J. Chem. Phys. **107**, 5332 (1997).

[5] S. Banerjee, S. S. Bhattacharyya, and S. Saha, Phys. Rev. A **49**, 1836 (1994).

[6] L. D. A. Siebbeles, J. M. Schins, W. J. van der Zande, J. A.

Beswick, and N. Halberstadt, Phys. Rev. A **45**, 4481 (1992).

[7] L. D. A. Siebbeles, J. M. Schins, W. J. van der Zande, J. Los, and M. Glass-Maujean, Phys. Rev. A **44**, 343 (1991).

[8] P. Senn, P. Quadrelli, and K. Dressler, J. Chem. Phys. **89**, 7401 (1988).

[9] P. Lambropoulas and X. Tang, in *Atoms in Intense Laser Fields*, edited by M. Gavrila (Academic, New York, 1992), p. 335.

[10] (a) S. Ghosh, S. S. Mitra, S. S. Bhattacharyya, and S. Saha, J. Phys. B **29**, 3109 (1996); (b) M. Protopapas and P. L. Knight, *ibid.* **28**, 4459 (1995).

[11] (a) K. Dressler and L. Wolniewicz, Can. J. Phys. **62**, 1706 (1984); (b) P. Quadrelli, K. Dressler, and L. Wolniewicz, J. Chem. Phys. **92**, 7461 (1990).

[12] (a) L. Wolniewicz and K. Dressler, J. Chem. Phys. **88**, 3861 (1988); (b) **85**, 2821 (1986); **82**, 3292 (1984); L. Wolniewicz, J. Mol. Spectrosc. **169**, 329 (1995); **174**, 132 (1995).

[13] W. Kolos, K. Szalewicz, and H. Z. Monkhorst, J. Chem. Phys. **84**, 3278 (1986); W. Kolos and L. Wolniewicz, *ibid.* **41**, 3663 (1964); A. L. Ford, A. M. Greenwalt, and J. C. Browne, *ibid.* **67**, 983 (1977).

[14] (a) J. W. Cooley, Math. Comput. **15**, 363 (1961); (b) W. Kolos and L. Wolniewicz, J. Chem. Phys. **50**, 3228 (1969); L. Wolniewicz and T. Orlikowski, J. Comput. Phys. **27**, 169 (1978).

[15] L. Wolniewicz, J. Chem. Phys. **51**, 5002 (1969).

[16] (a) L. Wolniewicz and K. Dressler, J. Mol. Spectrosc. **96**, 195 (1982); (b) L. Wolniewicz, *ibid.* **180**, 398 (1996).

[17] N. E. Greville, in *Mathematical Methods for Digital Computers*, edited by A. Ralston and H. S. Wilf (Wiley, New York, 1967), Vol. 2, p. 156.

[18] W. H. Press, S. A. Teukolsky, W. T. Vetterling, and B. P. Flannery, in *Numerical Recipes in Fortran* (Cambridge University Press, Cambridge, 1992), p. 70.